J|A|C|S
ARTICLES
Published on Web 07/14/2005

UV−Resonance Raman Thermal Unfolding Study of Trp-Cage Shows That It Is Not a Simple Two-State Miniprotein

Zeeshan Ahmed, Ilir A. Beta,† Aleksandr V. Mikhonin, and Sanford A. Asher*

Contribution from the Department of Chemistry, University of Pittsburgh, Pennsylvania 15260

Received February 1, 2005; E-mail: asher@pitt.edu

Abstract: Trp-cage, a synthetic 20 residue polypeptide, is proposed to be an ultrafast folding synthetic miniprotein which utilizes tertiary contacts to define its native conformation. We utilized UV resonance Raman spectroscopy (UVRS) with 204 and 229 nm excitation to follow its thermal melting. Our results indicate that Trp-cage melting is complex, and it is not a simple two-state process. Using 204 nm excitation we probe the peptide secondary structure and find the Trp-cage's α-helix shows a broad melting curve where on average four α-helical amide bonds melt upon a temperature increase from 4 to 70 °C. Using 229 nm excitation we probe the environment of the Trp side chain and find that its immediate environment becomes more compact as the temperature is increased from 4 to 20 °C; however, further temperature increases lead to exposure of the Trp to water. The χ^2 angle of the Trp side chain remains invariant throughout the entire temperature range. Previous kinetic results indicated a single-exponential decay in the 4−70 °C temperature range, suggesting that Trp-cage behaves as a two-state folder. However, this miniprotein does not show clear two-state behavior in our steady-state studies. Rather it shows a continuous distribution of steady-state spectral parameters. Only the α-helix melting curve even hints of a cooperative transition. Possibly, the previous kinetic results monitor only a small region of the Trp-cage which locally appears two-state. This would then argue for spatially decoupled folding even for this small peptide.

Introduction

The primary sequence of proteins encodes both the structure of the native and unfolded states, as well as the dynamics of the protein (un)folding processes.[1−16] Over the last 50 years significant efforts have been expended to elucidate the mechanisms of protein folding and unfolding. Part of this effort has examined the thermodynamic and kinetic behavior of small model systems such as the beta hairpins[17−20] and alanine-based α-helices (AP).[21−31]

These systems display secondary structure motifs that change with temperature. These simple systems also avoid tertiary structural motifs that could complicate the conformational dynamics of these pure secondary structure motifs. The secondary structure unfolding of these small peptides, such as the alanine-based helical peptides, involves thermally driven conformational changes of isolated peptide molecules in water, which melt from an α-helical conformation to a PPII conformation.[31,32] This conformational change is a property of the isolated peptide molecule and does not involve any tertiary-type interactions which may dominate (un)folding in larger proteins.

† Current address: Department of Physics, Kansas State University, Manhattan, KS 66506.

(1) Anfinsen, C. B. *Science* **1973**, *181*, 4096, 223−230.
(2) Chan, H. S.; Dill, K. A. *Proteins: Struct, Funct. Genet.* **1998**, *30*, 2−33.
(3) Dill, K. A. *Biochemistry* **1990**, *29*, 7133−7155.
(4) Jewett, A. I.; Pande, V. S.; Plaxco, K. W. *J. Mol. Biol.* **2003**, *326*, 247−253.
(5) Hardin, C.; Eastwood, M. P.; Prentiss, M.; Luthey-Schulten, Z.; Wolynes, P. G. *J. Comput. Chem.* **2002**, *23*, 138−146.
(6) Cleland, J. *Protein folding: in vivo and in vitro;* American Chemical Society: Washington, DC, 1993.
(7) Dill, K. A.; Alonso, D. O.; Hutchinson, K. *Biochemistry* **1989**, *28*, 5439−5449.
(8) Glaser, R. *Biophysics* Revised 5th ed.; Springer: New York, 2000.
(9) Alm, E.; Baker, D. *Proc. Natl. Acad. Sci. U.S.A.* **1999**, *96*, 11305−11310.
(10) Wolynes, P. G.; Onuchic, J. N.; Thirumalai, D. *Science* **1995**, *267*, 5204, 1619−1620.
(11) Pappu, R. V.; Srinivasan, R.; Rose, G. D. *Proc. Natl. Acad. Sci. U.S.A.* **2000**, *97*, 23, 12565−12570.
(12) Myers, J. K.; Oas, T. G. *Annu. Rev. Biochem.* **2002**, *71*, 783−815.
(13) Shortle, D. *Curr. Opin. Struct. Biol.* **1993**, *3*, 66−74.
(14) Bryngelson, J. D.; Wolynes, P. G. *J. Phys. Chem.* **1989**, *93*, 6902−6915.
(15) Hao, M.; Scheraga, H. A. *J. Phys. Chem.* **1994**, *98*, 9882−9893.
(16) Dobson, C. M.; Salij, A.; Karplus, M. *Angew. Chem., Int. Ed.* **1998**, *37*, 868−893.
(17) Muñoz, V.; Thompson, P. A.; Hofrichter, J.; Eaton, W. A. *Nature* **1997**, *390*, 196−199.
(18) Eaton, W. A.; Muñoz, V.; Thompson, P. A.; Henry, E. R.; Hofrichter, J. *Acc. Chem. Res.* **1998**, *31*, 745−753.
(19) Muñoz, V.; Henry, E. R.; Hofrichter, J.; Eaton, W. A. *Proc. Natl. Acad. Sci. U.S.A* **1998**, *95*, 5872−5879.
(20) Dinner, A. R.; Lazaridis, T.; Karplus, M. *Proc. Natl. Acad. Sci. U.S.A.* **1999**, *96*, 9068−9073.
(21) Thompson, P.; Eaton, W. A.; Hofrichter, J. *Biochemistry* **1997**, *36*, 9200−9210.
(22) Lednev, I. K.; Karnoup, Anton S.; Sparrow, M. C.; Asher, S. A. *J. Am. Chem. Soc.* **1999**, *121*, 8074−8086.
(23) Bolin, K. A.; Millhauser, G. L. *Acc. Chem. Res.* **1999**, *32*, 1027−1033.
(24) Garcia, A. E.; Sanbonmatsu, K. Y. *Proc. Natl. Acad. Sci. U.S.A.* **2002**, *99*, 5, 2782−2787.
(25) Andrew, C. D.; Warwicker, J.; Jones, G. R.; Doig, A. J. *Biochemistry* **2002**, *41*, 1897−1905.
(26) Lednev, I. K.; Karnoup, A. S.; Sparrow, M. C.; Asher, S. A. *J. Am. Chem. Soc.* **2001**, *123*, 2388−2392.
(27) Woutersen, S.; Hamm, P. *J. Chem. Phys.* **2001**, *114*, 2727.
(28) Clarke, D. T.; Doig, A. J.; Stapley, B. J.; Jones, G. R. *Proc. Natl. Acad. Sci. U.S.A.* **1999**, *96*, 7232−7237.
(29) Williams, S.; Causgrove, T. P.; Gilmanshin, R.; Fang, K. S.; Callender, R. H.; Woodruff, W. H.; Dyer, R. B. *Biochemistry* **1996**, *35*, 691−697.
(30) Ianoul, A.; Mikhonin, A.; Lednev, I. K.; Asher, S. A. *J. Phys. Chem. A* **2002**, *106*, 3621−3624.
(31) Asher, S. A.; Mikhonin, A. V.; Bykov, S. V. *J. Am. Chem. Soc.* **2004**, *126*, 27, 8433−8440.
(32) Tiffany, M. L.; Krimm, S. *Biopolymers* **1968**, *6*, 1379−1382.

Numerous experimental and computational investigations have probed the thermodynamic and kinetic behavior of these simple model systems.[17,21−24] Theoretical simulations of folding/unfolding have provided the most detailed microscopic understanding of the peptide's folding energy landscape.[21,22] At the same time sophisticated kinetic measurements have examined the earliest steps in the pure secondary structure unfolding process.[17,18,22,30]

To extend our understanding of secondary structure conformational changes to the corresponding phenomena in proteins it is essential to understand the role of tertiary contacts. Obviously we should start this investigation by examining small model protein systems in order to elucidate the impact of defined tertiary contacts such as hydrogen bonding and hydrophobic contacts on the secondary structure evolution.

In this regard, in this study we used UV resonance Raman spectroscopy (UVRS) to study the temperature dependence of the conformation of a 20-residue long miniprotein, Trp-cage synthesized by Neidigh et al.[33] which has the sequence N_1-LYIQWLKDG$_{10}$GPSSGRPPPS. Trp-cage was created during a de novo peptide design effort, which resulted from a study of a poorly folded 39-residue long saliva protein of a Gila monster.[33] Using an iterative design effort with selective mutations and truncations, different protein variants were created and their folded states were characterized using NMR and circular dichroism spectroscopy (CD). Trp-cage, originally referred to as Tc5b, showed the most structure, displaying a cage of hydrophobic residues surrounding the Trp side chain. Trp-cage was found to be 95% folded under physiological conditions.[33] Trp-cage, which consists entirely of natural amino acids appears to exhibit elements of tertiary structure even though it has no disulfide bridges, metal ion chelation motifs, or stabilization through oligomerization.[34] In addition, Trp-cage possesses a hydrophobic core, which surrounds the Trp side chain and shields it from the aqueous environment.

The NMR and CD Trp-cage data of Neidigh et al. suggested a simple two-state unfolding mechanism.[33,34] Qiu et al. using the intrinsic fluorescence of Trp determined the folding time to be about 4 μs, which makes Trp-cage the fastest folding polypeptide possessing tertiary contacts.[35]

This is especially noteworthy since the fundamental speed limit on protein folding has been estimated to give rise to a folding time of $\sim(N/100)$ μs, where N is number of protein residues.[36−40] This would result in a theoretical folding speed limit for Trp-cage of $\sim$0.2 μs, only 20 times faster than the experimentally determined folding time. This implies an almost optimized energy landscape for this peptide, where folding is largely dominated by free polymer diffusion.[35]

Several groups recently reported theoretical simulations of Trp-cage folding.[41−48] For example, Simmerling et al.[41] in their all atom molecular dynamics simulation, presented a detailed molecular picture of Trp-Cage's folding dynamics. Their simulation calculated a native state topology consistent with the NMR structure of Neidigh et al.[33] Their simulation at 325 K, which modeled the folding of Trp-cage, found that the extended Trp-cage conformation converges to a native state topology within 20 ns. Snow et al.[43] carried out stochastic dynamics simulations over a total modeled folding time of 100 μs and found that the unfolded state retains features similar to the native state topology.

In this work we used UV resonance Raman spectroscopy to examine the temperature dependence of the Trp-cage conformation. We studied the protein secondary structure by exciting within the amide $\pi\rightarrow\pi^*$ transition with 204 nm excitation[22] and used 229 nm excitation to excite within the aromatic ring $\pi\rightarrow\pi^*$ transitions to study the Trp[49] and Tyr[50,51] aromatic side chains. Our results indicate that Trp-cage's thermal unfolding is much more complex than suggested by previous studies.

Experimental Section

The UV resonance Raman (UVRR) spectrometer has been described in detail elsewhere.[22] Briefly, 204 nm UV light was obtained by generating the fifth anti-Stokes Raman harmonic of the third harmonic of a Nd:YAG laser (Coherent, Infinity). The 229 nm excitation was produced by an intracavity frequency doubling of an Ar^+ laser (Coherent, FReD 400). The sample was circulated in a free surface, temperature-controlled stream. A 180° backscattering geometry was used for sampling. The collected light was dispersed by a double monochromator onto a back thinned CCD camera (Princeton Instruments-Spec 10 System).

Polyproline (MW 8900) and AcTrpEE (Trp monomer) were acquired from Sigma-Aldrich and used at 12 and 2 μM concentrations, respectively, for UV absorption measurements. A solution of 112 μM polyproline, 50 μM Trp monomer, and 0.3 M ClO_4^- was used for the 229 nm excited UVRR temperature dependence measurements. The 21-residue long alanine-based helical peptide AP[22] was obtained from the Pittsburgh Peptide Synthesis Facility (PPSF, >95% purity) and used at 2 mg/mL concentrations for determining the 204 nm Raman cross sections. A concentration of 1 mg/mL of Trp-cage (PPSF, >95% purity) at pH 7 was used for the 204 nm excitation temperature dependence study, while a 2 mg/mL concentration was used for the 229 nm excitation temperature dependence study. Previous work indicates there is no significant concentration dependence[33] of Trp-cage's conformation between 1 and 7 mg/mL at pH 7.

Spectra measured at 20 °C after the elevated temperature measurements were essentially identical to those prior to the temperature increase, indicating no significant sample photo- or thermal degradation or irreversible aggregation. Raman spectra were normalized relative to the peak height of the 932 cm^{-1} ClO_4^- band. 0.1 M perchlorate concentrations were used in the Trp-cage samples, whereas, 0.2 M concentrations were used for the AP peptide samples. The pH was adjusted by adding small aliquots of HCl or NaOH.

(33) Neidigh, J. W.; Fesinmeyer, R. M.; Andersen, N. H. *Nat. Struct. Biol.* **2002**, *9*, 6, 425−430.
(34) Gellman, S. H.; Woolfson, D. N. *Nat. Struct. Biol.* **2002**, *9*, 6, 408−410.
(35) Qiu, L.; Pabit, S. A.; Roitberg, A. E.; Hagen, S. J. *J. Am. Chem. Soc.* **2002**, *124*, 12952−12953.
(36) Hagen, S. J.; Hofrichter, L.; Szabo, A.; Eaton, W. A. *Proc. Natl. Acad. Sci. U.S.A.* **1996**, *93*, 11615−11617.
(37) Pascher, T.; Chesick, J. P.; Winkler, J. R.; Gray, H. B. *Science* **1996**, *27*, 5255, 1558−1560.
(38) Kubelka, J.; H., James; Eaton, W. A. *Curr. Opin. Struct. Biol.* **2004**, *14*, 1, 76−88.
(39) Hagen, S. J.; Hofrichter, L.; Eaton, W. A. *J. Phys. Chem. B* **1997**, *101*, 2325−2365.
(40) Kubelka, J.; Eaton, W. A.; Hofrichter, J. *J. Mol. Biol.* **2003**, *329*, 625−630.
(41) Simmerling, C.; Strockbine, B.; Roitberg, A. E. *J. Am. Chem. Soc.* **2002**, *124*, 11258−11259.
(42) Roitberg, A. E. Personal communication.
(43) Snow, C. D.; Zagrovic, B.; Pande, V. S. *J. Am. Chem. Soc.* **2002**, *124*, 14548−14549.
(44) Chowdhury, S.; Lee, M. C.; Xiong, G.; Duan, Y. *J. Mol. Biol.* **2003**, *327*, 711−717.
(45) Zhou, R. *J. Mol. Graphics Modell.* **2004**, *22*, 451−462.
(46) Zhou, R. *Proc. Natl. Acad. Sci. U.S.A.* **2003**, *100*, 23, 13280−13285.
(47) Chowdhury, S.; Lee, M. C.; Xiong, G.; Duan, Y. *J. Phys. Chem. B* **2004**, *108*, 13855−13865.
(48) Pitera, J. W.; Swope, W. *Proc. Natl. Acad. Sci. U.S.A.* **2003**, *100*, 13, 7587−7592.
(49) Sweeny, J. A.; Asher, S. A. *J. Phys. Chem.* **1990**, *94*, 12, 4784−4791.
(50) Ludwig, M.; Asher, S. A. *J. Am. Chem. Soc.* **1988**, *110*, 1005−1011.
(51) Chi, Z.; Asher, S. A. *Biochemistry* **1998**, *37*, 2865−2872.

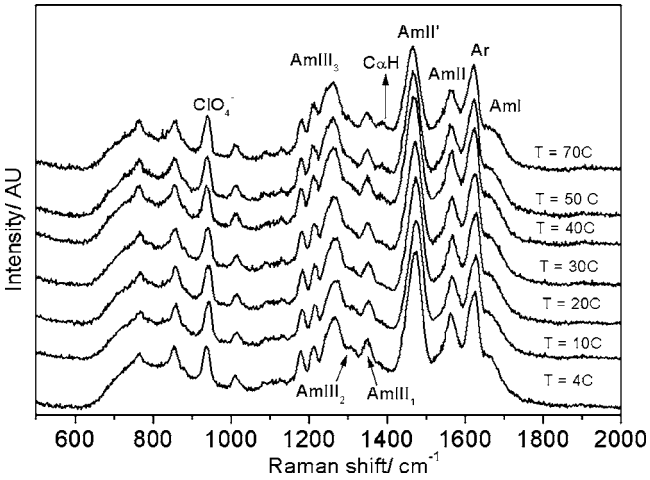

Figure 1. 204 nm UV resonance Raman spectra of Trp-Cage measured between 4 and 70 °C. Three 5 min spectra were summed and scaled to the intensity of the 932 cm^{-1} perchlorate band. The bands arise mainly from amide vibrations except for a few which derive from aromatic ring vibrations of Trp and Tyr residues.

Results and Discussion

204 nm Excitation Temperature Dependence. We examined the temperature dependence of Trp-Cage's backbone conformation by measuring 204 nm UV resonance Raman spectra between 4 and 70 °C (Figure 1). The spectra show bands mainly arising from amide vibrations, with smaller contributions from the Trp and Tyr aromatic ring vibrations. The Amide I band (AmI) at ∼1662 cm^{-1} is predominantly a C═O stretching vibration[52,53] and occurs as a shoulder on the intense aromatic amino acid band at ∼1620 cm^{-1}. The Amide II band (AmII) at 1564 cm^{-1} involves C—N stretching with some N—H bending.[52,53] The AmII' band of proline[54−59] located at 1474 cm^{-1} is almost a pure C—N stretch, while the C_α—H bending band is located at 1386 cm^{-1}. The presence of the resonance enhanced C_α—H bending band has previously been correlated with the presence of nonhelical peptide bond conformations.[52,60]

The Amide III region has recently been examined and reassigned.[61−65] Trp-cage shows the following bands in this region: the Amide III_3 band at 1264 cm^{-1} (predominantly C−N stretching and N−H bending[52,53,64]), a shoulder at 1312 cm^{-1} ($AmIII_2$), and an $AmIII_1$ band at 1348 cm^{-1}.

We deconvoluted these measured spectra into a sum of a minimum number of Voight bands by using the peak fitting routine in Grams software (Galactic Industries Corporation, Grams version 5). A typical example of such a fit is shown in Figure 2 for the 4 °C 204 nm spectrum. The assignments and frequencies of the deconvoluted bands are listed in Table 1.

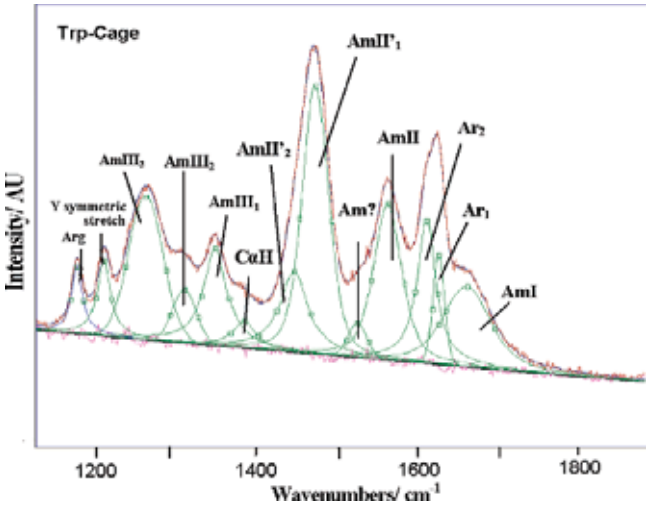

Figure 2. Spectral deconvolution of 4 °C 204 nm UVRR Trp-cage spectra with Voight bands. The excellence of the fit is evident from the flat residual displayed underneath.

Table 1. Spectral Assignment of Trp-Cage UVRR Spectra

band	frequency (cm^{-1})
Amide I	1662
Aromatic I	1627
Aromatic II	1611
Amide II	1564
Amide ?	1526
Amide II_1'	1474
Amide II_2'	1447
C_α-H (sb)	1386
Amide III_1	1348
Amide III_2	1312
Amide III_3	1264
Tyr (Y) symmetric stretch	1210
Arg side chain	1178

We observe numerous temperature-induced spectral changes. For example the proline AmII′ band frequency downshifts from 1474 to 1464 cm^{-1} as the temperature increases from 4 to 70 °C. Furthermore, we find that the $AmIII_3$ band monotonically downshifts from 1264 cm^{-1} at 4 °C to 1256 cm^{-1} at 70 °C. Previously, Lednev et al.[22] observed a similar temperature dependence of the $AmIII_3$ band in AP peptide.[22,31] As shown in detail by Mikhonin et al.[64] the $AmIII_3$ band shift results from the weakening of the peptide bond-water hydrogen bonding (N−H····O) at higher temperatures,[31] similar to that observed in *N*-methyl acetamide.[66−68] This is associated with the typical weakening of hydrogen bonding between the protein peptide bonds and the water environment which occurs as the temperature increases.[31]

The difference spectrum between the 4 and 70 °C spectra shown in Figure 3 shows a decrease in the intensity of a triplet of bands in the AmIII region centered at ∼1300 cm^{-1} which derives from the α-helical conformation.[22,64] The decrease in the intensity of the triplet indicates partial melting of the α-helices as the temperature is increased from 4 to 70 °C. The

(52) Chi, Z.; Chen, X. G.; Holtz, J. S. W.; Asher, S. A. *Biochemistry* **1998**, *37*, 2854−2864.
(53) Mirkin, N. G.; Krimm, S. *J. Mol. Struct.* **1996**, *377*, 219.
(54) Caswell, D. S.; Spiro, T. G. *J. Am. Chem. Soc.* **1987**, *109*, 2796−2800.
(55) Rippon, W. B.; Koenig, J. L.; Walton, A. G. *J. Am Chem. Soc.* **1970**, *92*, 7455−7459.
(56) Mayne, L.; Hudson, B. *J. Phys. Chem.* **1987**, *91*, 4438−4440.
(57) Dorman, D. E.; Torchia, D. A.; Bovey, F. A. *Macromolecules* **1973**, *6*, 80−82.
(58) Harhay, G. P.; Hudson, B. S. *J. Phys. Chem.* **1991**, 3511−3513.
(59) Swenson, C. A. *Biopolymers* **1970**, *10*, 2591−2596.
(60) Wang, Y.; Purrello, R.; Jordan, T.; Spiro, T. G. *J. Am. Chem. Soc.* **1991**, *113*, 6359−6368.
(61) Diem, M.; Lee, O.; Roberts, G. M. *J. Phys. Chem.* **1992**, *96*, 548.
(62) Lee, S. H.; Krimm, S. *Biopolymers* **1998**, *46*, 283.
(63) Lee, S. H.; Krimm, S. *Chem. Phys.* **1998**, *230*, 277.
(64) Mikhonin, A. V.; Ahmed, Z.; Ianoul, A.; Asher, S. A. *J. Phys. Chem. B* **2004**, *108*, 19020−19028.
(65) Overman, S. A.; Thomas, G. J., Jr. *Biochemistry* **1998**, *37*, 5654−5665.
(66) Torii, H. *J. Phys. Chem. A* **2004**, *108*, 7272−7280.
(67) Besley, N. A.; Oakley, M. T.; Cowan, A. J.; Hirst, J. D. *J. Am. Chem. Soc.* **2004**, *126*, 13502−13511.
(68) Triggs, N. E.; Valentini, J. J. *J. Phys. Chem.* **1992**, *96*, 6922−6931.

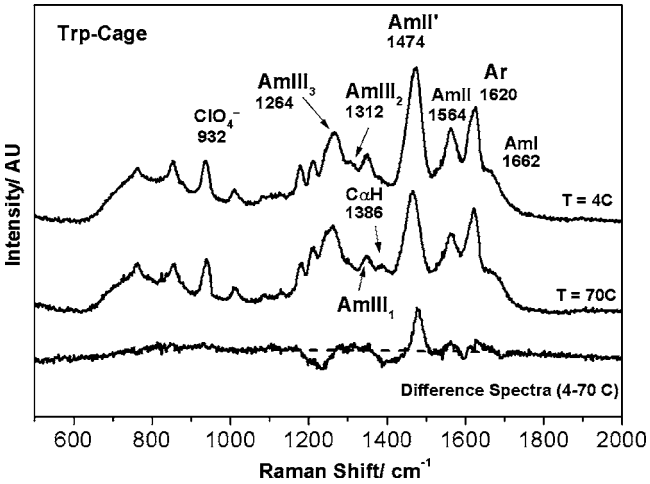

Figure 3. 204 nm UV resonance Raman spectra of Trp-cage at 4 and 70 °C and their difference spectra. The difference spectra show a decrease in the intensity of a triplet in the AmIII frequency region indicating a loss of α-helix with increasing temperature. The trough in the $C_\alpha-H_b$ (1386 cm^{-1}) and the $AmIII_3$ (1220 cm^{-1}) region also indicates α-helix melting. The intensity of the AmII′ proline band also decreases at higher temperatures.

trough in the $C_\alpha-H_b$[22,31,60] region at ∼1386 cm^{-1} and the deep trough at ∼1220 cm^{-1} for the $AmIII_3$ region further confirms the melting of α-helical residues to non-α-helical conformations.[31]

The difference spectra also indicate a 10 cm^{-1} downshift and a significantly decreased Raman intensity for the proline AmII′ band as the temperature is increased. This suggests either an environmental[69] or conformational[54] change for the proline imide bond(s). The frequency position of AmII′ of proline has been thought to be indicative of cis−trans isomerization of the proline imide bond. Caswell and Spiro[54] reported that, in polyproline, the AmII′ band downshifted from 1465 to 1435 cm^{-1} upon conversion of polyproline from the PPII (trans) to PPI (cis) conformation. It should, however, be noted that their conclusions were disputed by Harhay and Hudson,[58] who reported that at 200 nm excitation, simple X-Pro dipeptides did not show changes in their AmII′ band frequencies when their cis content was increased via a pH increase; furthermore, Harhay and Hudson[58] attributed the decreases in proline AmII′ band intensities to pH-induced bathochromic shifts in the UV absorption.

An alternative interpretation of the AmII′ spectral frequency dependence was suggested by Takeuchi et al.[69] who proposed that the observed shift in the band position could be due to differences in the hydrogen bonding environment of the imide bond. The authors reported that in aprotic solvents such as acetonitrile the proline AmII′ band is downshifted by 25−30 cm^{-1} as compared to an aqueous solution, suggesting solvent-imide hydrogen bonding is primarily responsible for the observed changes in band position. In non-hydrogen bonding environments the AmII′ band occurs around 1440 cm^{-1}, while strong hydrogen bonding upshifts the band to 1480 cm^{-1}.[69] Their results would suggest that at 4 °C the Trp-cage's prolines (1474 cm^{-1}) are strongly hydrogen bonded, while at higher temperatures the imide-water hydrogen bonds are weakened.

Proline-Trp Excitonic Interactions. The decrease in the Raman intensity of the AmII′ band appears to result from excitonic interactions between the Trp side chain and proline imide bond. As shown by the Figure 4 absorption spectrum of solutions of polyproline, the addition of Trp monomer decreases the polyproline's 204 nm extinction coefficient by 6%.[70] Presumably this hypochromism results from interactions between the $\pi\rightarrow\pi^*$ transition moments of the proline peptide bond and the $\pi\rightarrow\pi^*$ transition moments of the Trp aromatic ring.

We modeled the Trp-polyproline spectral changes by subtracting the absorption of polyproline from the Trp-polyproline mixture absorption spectrum. As shown in the Figure 4 inset, a scaling of 0.91 for the subtracted polyproline spectrum allows us to recover the B_b absorption curve of Trp between ∼204 and 229 nm (see below). The impact of excitonic interactions occurs mainly below 204 nm and appears to involve mainly the polyproline transition. It is clear from the inset difference spectrum that the ∼220 nm B_b band of Trp is not affected by the excitonic interactions with proline.

We, thus, expect changes in the excitonic interaction to have no significant impact on the Trp band intensities (to the extent resonance enhancement is dominated by the Trp's B_b transition). The situation, however, is somewhat complex for 204 nm excitation Raman spectra, since this excitation occurs on the blue edge of the B_b absorption, between the B_b and B_a electronic transitions.[49] This is a region where a minimum in intensities occurs and the excitation profile dispersion is small.[49] Thus, excitation in this region is expected to be somewhat insensitive to shifts in absorption bands. However, Sweeney and Asher[49] noted evidence for destructive interference for Trp intensities due to the contribution of the higher energy B_a transition. This would then lead to a dependence on absorbance changes for the B_a transition, which could be impacted by excitonic interactions with prolines. Although the situation appears complex, the best overall estimate would be that the Trp intensities excited at 204 nm will show less intensity dependencies for change in excitonic interactions than would the proline Raman intensities. In addition, the intensities will be relatively insensitive to Trp B_b absorption band shifts.

Figure 5A shows that the AmII′ Raman band of proline excited at 204 nm shows a monotonic 33% intensity decrease as the temperature increases from 4 to 70 °C. These results indicate that a gradual conformational change occurs that causes hypochromism of the AmII′ of proline's resonance Raman intensities. This probably results from an increase in Trp-proline excitonic interactions either because the proline(s) and tryptophan become situated closer together or because of a change in the alignments of proline and Trp transition dipole moments.[71] Most likely the packing of prolines about the Trp becomes tighter as the temperature increases. As expected from the discussion above, for 204 nm excitation there are no intensity changes for the Trp Raman bands with temperature (not shown).

α-Helix Melting. Changes in the observed Raman intensity of the $C_\alpha-H$ bending and the $AmIII_3$ band result from decreases in the number of α-helical amide bonds as the temperature increases (Figures 3 and 5). We can most easily estimate the change in the number of α-helical amide bonds from the

(69) Takeuchi, H.; Harada, I. *J. Raman Spectrosc.* **1990**, *21*, 509−515.

(70) A 6% decrease in absorption would result in a ∼12% decrease in the resonance Raman cross sections (RCS roughly scale as the square of extinction coefficient). In the case of Trp-cage the AmII′ band intensity decreases by ∼33% between 4 and 70 °C.

(71) Cantor, C. R.; Schimmel, P. R. *Biophysical Chemistry*; Freeman and Compant: San Francisco, CA, 1980; Vol. 1.

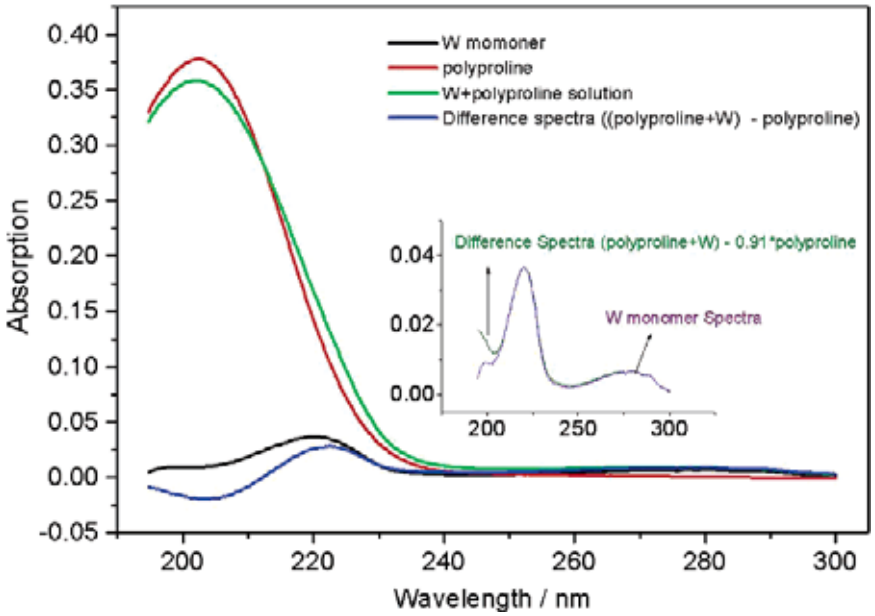

Figure 4. UV absorption spectra of Trp monomer (AcTrpEE), polyproline, and a solution of Trp (W) and polyproline, and the (Polyproline + Trp) − Trp difference spectrum. Inset shows Trp monomer spectra and difference spectra of (Polyproline +Trp) minus 0.91*Polyproline.

increased intensity of the C_α−H bending band resonance Raman band, which only occurs in non-α-helical conformations.[31,60] This band is well isolated in the spectra. A similar analysis using the decreased intensity of the AmIII bands is less reliable due to overlap of the AmIII bands from the folded and unfolded states.[64] Little α-helix melting occurs up until ∼25 °C, and the melting curve shows a rough T_M at ∼40 °C.

We can quantitate the change in the number of α-helical amide bonds by using the Raman cross sections of the C_α−H bending band from a 21-residue, alanine-based, mostly α-helical peptide known as AP[22] (Figure 6); we are utilizing the assumption that the Trp-cage's unfolded segment C_α−H bending bands have Raman cross sections similar to those of the unfolded PPII conformation of AP.[31] This is a reasonable estimate since C_α−H bending bands have similar cross sections in the PPII and extended β-sheet strand conformations;[31,52,64] we expect similar couplings of C_α−H and N−H for peptide bonds with similar Ψ angles.[72]

AP is ∼95% PPII at 60 °C.[22,31] Thus, the 204 nm excited 60° C AP spectra are dominated by the PPII conformation, with only a small contribution from the α-helical state. The 204 nm AP spectrum in Figure 6 shows a single AmI band at ∼1660 cm^{-1}. The AmII band is located at ∼1555 cm^{-1}, while the C_α−H sb appears as a doublet at 1370 and 1394 cm^{-1}. The $AmIII_3$ band is located at ∼1250 cm^{-1}, the $AmIII_2$ band at 1304 cm^{-1}, while the $AmIII_1$ band is found at ∼1336 cm^{-1}. The origins of the resonance-enhanced amide III bands and PPII spectral markers have been extensively described by Mikhonin[64] and Asher et al.[31]

Using Dudik et al.'s data[73] for the absolute Raman cross section of the 932 cm^{-1} band of perchlorate at 204 nm excitation, we calculated the Raman cross sections for AP:

$$\sigma_A = (I_A N_{ClO4^-}\sigma_{ClO4^-})/(n_A N_{AP} I_{ClO4^-}) \quad (1)$$

where, σ_A and σ_{ClO4^-} are the Raman cross sections of an amide band and the 932 cm^{-1} perchlorate band, respectively. N_{ClO4^-} and N_{AP} are the number of perchlorate and AP molecules in the scattering volume, respectively. I_{ClO4^-} is the perchlorate band (932 cm^{-1}) intensity, while I_A is the intensity of the amide band. n_A is the number of amide peptide bonds in AP which contribute to the intensity I_A of the concerned band. The calculated cross sections of AP amide bands are listed in Table 2. Using the C_αH band cross sections we calculated the number of nonhelical amide bonds in Trp-cage as

$$n_A = (I_{C\alpha H} N_{ClO4^-}\sigma_{ClO4^-})/(\sigma_{C\alpha H} N_P I_{ClO4^-}) \quad (2)$$

where N_P are the number of molecules of Trp-cage in the scattering volume. We estimate that at 4 °C Trp-cage has six, nonprolyl, nonglycine amide bonds in a nonhelical, PPII conformation. Hence there are six nonprolyl, nonglycine amide bonds in an α-helical conformation. From the spectral intensity changes plotted in Figure 5B we can calculate the number of α-helix peptide bonds which melt as

$$\delta n_A = (-\delta I_{C\alpha H} N_{ClO4^-}\sigma_{ClO4^-})/(\sigma_{C\alpha H} N_P) \quad (3)$$

Where δn_A is number of α-helical bonds lost or gained and $\delta I_{C\alpha H}$ is the change in normalized C_α−H bending band intensity. The 70% increase in the C_α−H bending band intensity suggests approximately four more amide bonds contribute to the C_α−H bending band intensity at 70 °C then at temperatures below 30 °C.

The observed decrease in the helical content is likely associated with a shift in the Trp-cage equilibrium toward non-native, nonhelical states, rather than a shortening of the α-helices in their native conformation. We envision that Trp-cage flickers between native and unfolded conformations and that the intensity decrease results from a smaller duty cycle for the native state α-helix length; very short α-helices are inherently unstable.[22]

Our α-helix melting curve appears broader than the melting curve determined by Neidigh et al.[33] Their CD and NMR data

(72) Asher, S. A.; Ianoul, A.; Mix, G.; Boyden, M. N.; Karnoup, A.; Diem, M.; Schweitzer-Stenner, R. *J. Am. Chem. Soc.* **2001**, *123*, 11775−11781.
(73) Dudik, J. M.; Johnson, C. R.; Asher, S. A. *J. Chem. Phys.* **1985**, *82*, 1732.

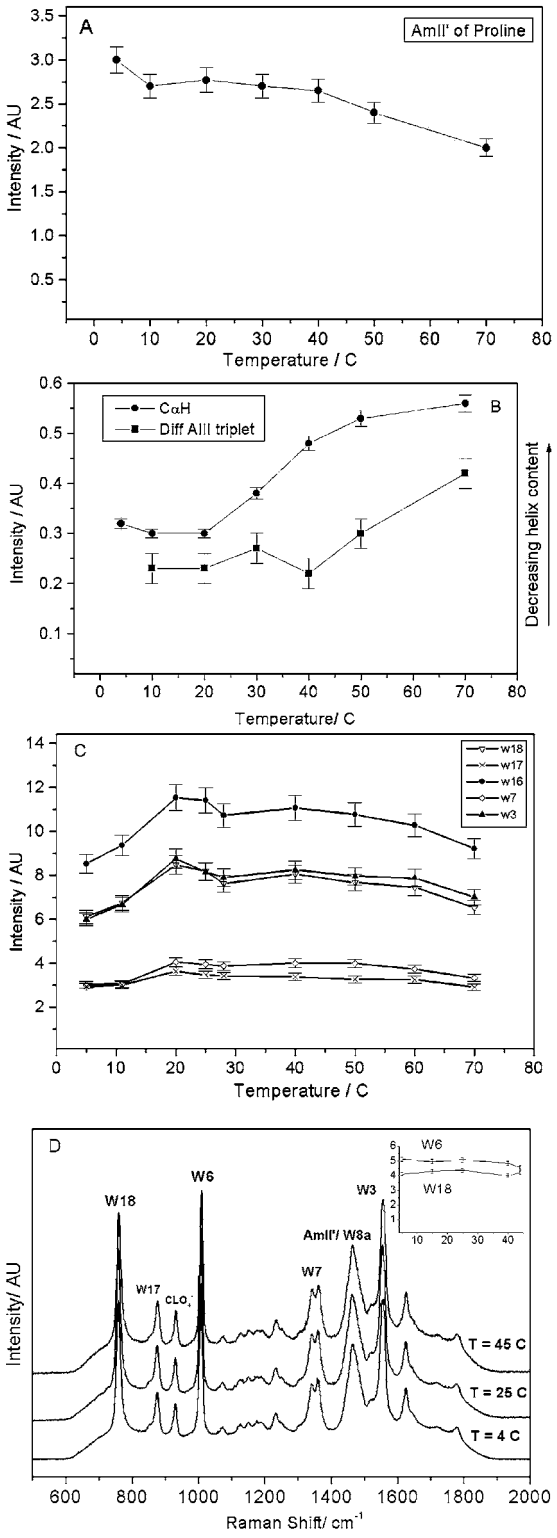

Figure 5. (A) Temperature dependence of 204 nm excited Raman intensity of proline AmII′ band. (B) Temperature dependence of the $C_\alpha-H$ symmetric bending band intensity and the α-helical AmIII band triplet intensity. The triplet intensity is extracted from temperature difference spectrum. Increasing $C_\alpha H$ and AmIII triplet intensities indicate loss of α-helicity at higher temperatures. (C) Temperature dependence of the relative Raman intensities of different Trp bands: W18 (▼, 765 cm^{-1}), W17 (×, 884 cm^{-1}), W16 (●, 1014 cm^{-1}), W7 (◇, 1365 cm^{-1}), W3 (▲ 1558 cm^{-1}). (D) 229 nm UV resonance Raman spectra of Trp monomers in polyproline solution at different temperatures. The spectra show bands arising from the resonance-enhanced Trp along with AmII′ of proline which overlaps with the W8a band of Trp. Temperature dependence of W6 and W18 bands of Trp is displayed in the inset.

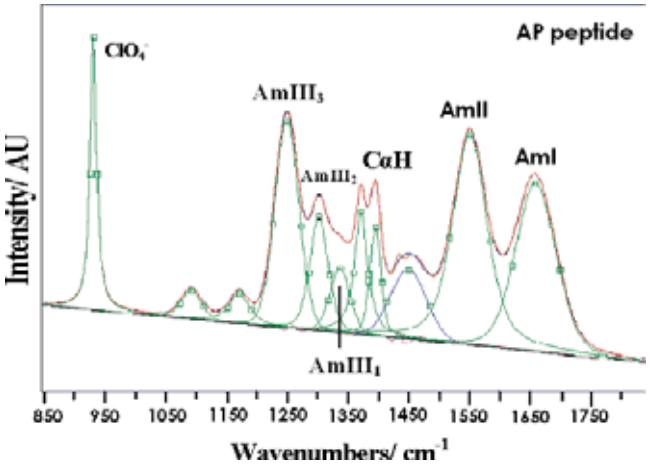

Figure 6. 204 nm UV resonance Raman spectrum of AP peptide at 60 °C. The measured spectra are deconvoluted into a sum of Voight bands. At 60 °C AP is 95% PPII.

Table 2. Amide Cross Sections of AP Peptide

band	cross section [mbarn/(molecule*bond*sr)] at 204 nm
Amide II	17
Amide III_2	10
Amide III_3	20
$C_\alpha-H$ (1370 cm^{-1})	14
$C_\alpha-H$ (1394 cm^{-1})	12

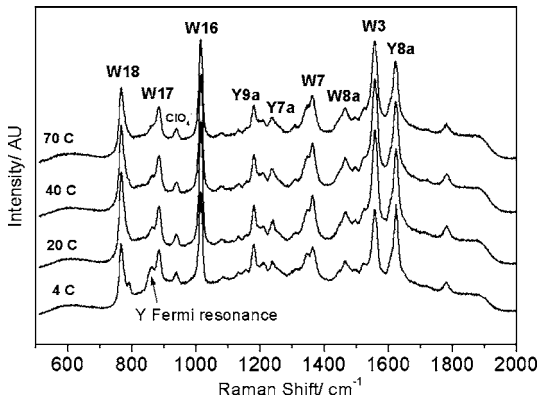

Figure 7. 229 nm UV resonance Raman spectra of Trp-Cage at different temperatures. Three spectra accumulated for 10 min each were summed and normalized to the 932 cm^{-1} perchlorate band intensity. The spectra show bands arising from the resonance-enhanced Trp and Tyr ring vibrations.

suggested a cooperative melting of the helix, while our UVRR spectra show a broader α-helix melting curve with little or no helix melting at temperatures below ~25 °C. The differences probably derive from the fact that their NMR data monitors the melting of both the amide backbone and the side chain conformations. In addition, Neidigh et al.'s CD data are confounded by contributions from the Trp side chain CD signals.[33] In contrast, our Figures 1 and 3 data report directly on the melting of the α-helices.

Trp and Tyr Water Exposure. We examined the environment of the Trp and Tyr residues of Trp-cage by measuring the temperature dependence of the 229 nm UVRR spectra of Trp-cage between 4 and 70 °C (Figures 5 and 7). The spectra are dominated by the in-plane aromatic ring vibrations of Trp and Tyr. The Trp bands appear at 766 (W18), 884 (W17), 1014

(W16), 1344 (W7), 1363 (W7), and 1558 cm^{-1} (W3), while those of Tyr are observed at 863 (Y Fermi resonance[49]), 1183 (Y9a), 1212 (Y7a), and 1627 cm^{-1} (Y8a). We do not observe any significant frequency shifts of the Trp and Tyr bands as the temperature increases. We determined the Trp and Tyr relative Raman cross sections from the ratio of the peak heights of the Trp and Tyr bands relative to that of the 932 cm^{-1} ClO_4^- band.

The Trp-cage Tyr intensities do not vary by more than 5% from 4 to 70 °C. Boyden et al.[74] previously reported that Tyr monomers in aqueous solutions show a cross section decrease with increasing temperature due to a temperature-induced decrease in the molar absorptivity of the resonant 220 nm absorption band.[74] The lack of an observed monotonic decrease in the Tyr intensities indicates a compensating Trp-cage conformation-induced intensity increase. However, we recently demonstrated that interactions between Tyr and polyproline give rise to blue shifts[75] in the Tyr resonant 220 nm absorption band. This suggests that these Tyr-proline excitonic interactions decrease as the temperature increases.

As shown in Figure 5C, the relative Raman intensities of the Trp bands increase by ~35% as the temperature increases from 4 °C to 20 °C and then steadily decrease as temperature further increases to 70 °C. Boyden et al.[74] showed that the Raman cross sections of monomeric Trp's in pure water do not show any appreciable temperature dependence. In contrast, we earlier demonstrated that the Raman cross sections of the Trp bands depend on the exposure of the indole ring to water due to the blue shifting of the ~220 nm absorption band upon water exposure.[76] Since 229 nm excitation occurs on the red edge of the Raman excitation profiles, a blue shift in the absorption band decreases the 229 nm Raman cross sections.[74,76] This intensity dependence can thus be used to monitor the solvent exposure of the Trp side chain by measuring changes in their relative Raman cross sections.[76,77]

Since, as discussed above, we expect no impact on the B_b transition from proline excitonic interactions, we expect that the Trp 229 nm intensity changes primarily result from changes in solvent exposure. This is especially clear from the Figure 5D 229 nm excited UV Raman spectrum of a sample containing Trp and polyproline which demonstrates a negligible Trp band temperature dependence.

The W17 band of Trp has been shown by Miura et al.[78] to be sensitive to the hydrogen bonding of indole's N−H. If the N−H is free of hydrogen bonding the W17 appears at 883 cm^{-1}, while strong hydrogen bonding of the indole N−H, downshifts the band to 871 cm^{-1}.[78] At 4° C we observe the W17 band at 884 cm^{-1} which remains more or less invariant as the Trp-cage is heated (Figure 7). The band frequency suggests that the indole does not hydrogen bond within the temperature range examined here. Furthermore, a lack of hydrogen bonding is known to blue shift the Trp excitation profiles, thereby diminishing the 229 nm excited UVRR intensities.[79,80] This is consistent with our measured Trp Raman cross sections at 4 °C which are lower than what would be expected even for a fully exposed Trp ring.

The temperature-induced intensity increases to 20 °C followed by the decrease suggests that the Trp initially becomes less exposed to water and then as the temperature further increases, its water exposure increases. This occurs in an environment where the Trp's N−H is incapable of hydrogen bonding. These changes are quite gradual with very broad transitions. The loss of exposure to water was also evident in the apparent increased excitonic interactions which resulted in a smaller proline AmII′ intensity at higher temperatures as discussed above.

The W7 band is a Fermi doublet with bands appearing at ~1360 and 1340 cm^{-1}. The ratio of 1360/1340 cm^{-1} band intensities, the R value is known to be indicative of hydrophobicity of the Trp's immediate environment. R values greater than one suggest a hydrophobic environment akin to that of aliphatic alkanes. A value of about one suggests an aromatic type environment, while values less than one suggest an aqueous environment.[81−85] At 4 °C the R value is around 1.8 (±0.1) and remains more or less invariant as the temperature is increased suggesting an invariant hydrophobic environment persists in Trp-cage at all temperatures.

Taken together the R-value analysis and the changes in the Trp band intensities tell us that the Trp ring is always in a hydrophobic environment which has a significant solvent accessibility. The Trp N−H is not hydrogen bonded at any temperature. The minimum solvent accessibility occurs at ~20 °C. The solvent accessibility at 70 °C is less than that at 4 °C.

We also examined the W3 band of Trp side chain. The position of this band correlates with the absolute value of the χ^2 dihedral angle of the Trp side chain involving $C_2-C_3-C_\beta-C_\alpha$ linkage.[86] The W3 band is positioned at 1558 cm^{-1} at 4 °C and does not vary to any significant degree as the temperature is increased. According to the data of Miura et al.[86] the band position here suggests a $|\chi^2|$ angle of ~110°. The invariance of the χ^2 suggests that Trp's conformation does not vary to any significant extent as the temperature is increased. This demonstrates that the indole's geometry with respect to the linkage to the peptide backbone is constant.

Conclusion

Trp-cage was selectively probed using 204 and 229 nm UV Raman excitation. We observe a broad melting transition of the α-helix with no significant α-helix melting until ~30 °C. On the average, four α-helical residues melt between 40 and 70 °C. Most likely, at higher temperatures, the Trp-cage conformation flickers between a native and a non-native, nonhelical state; the observed change in helicity is probably due to a smaller duty cycle for the native α-helix length.

The decreased proline intensities indicate a strengthening of proline(s)-Trp excitonic interactions with temperature indicating a more compact hydrophobic core. The 229 nm Trp Raman intensity changes are not monotonic. They show a maximum

(74) Boyden, M. N.; Asher, S. A. *Biochemistry* **2001**, *40*, 13723−13727.
(75) Ahmed, Z.; Asher, S. A. Manuscript in preparation.
(76) Chi, Z.; Asher, S. A. *J. Phys. Chem. B* **1998**, *102*, 9595−9602.
(77) Chi, Z.; Asher, S. A. *Biochemistry* **1999**, *38*, 8196−8203.
(78) Miura, T.; Takeuchi, H.; Harada, I. *Biochemistry* **1988**, *27*, 88−98.
(79) Mukerji, I.; Spiro, T. G. *Biochemistry* **1994**, *33*, 13132−13139.
(80) Rodgers, K. R.; Su, C.; Subramaniam, S.; Spiro, T. G. *J. Am. Chem. Soc.* **1992**, *114*, 3697−3709.
(81) Harada, I.; Miura, T.; Takeuchi, H. *Spectrochim. Acta* **1986**, *42A* (2/3), 307−312.
(82) Hideo, T.; Nemoto, Y.; Harada, I. *Biochemistry* **1990**, *29*, 1572−1579.
(83) Kochendoerfer, G. G.; Kaminaka, S.; Mathies, R. A. *Biochemistry* **1997**, *36*, 13153−13159.
(84) Hasmimoto, S.; Obata, K.; Takeuchi, H.; Needleman, R.; Lanyi, J. K. *Biochemistry* **1997**, *36*, 11583−11590.
(85) Miura, T.; Takeuchi, H.; Harada, I. *Biochemistry* **1988**, *27*, 88−94.
(86) Miura, T.; Takeuchi, H.; Harada, I. *J. Raman Spectrosc.* **1989**, *20*, 667−671.

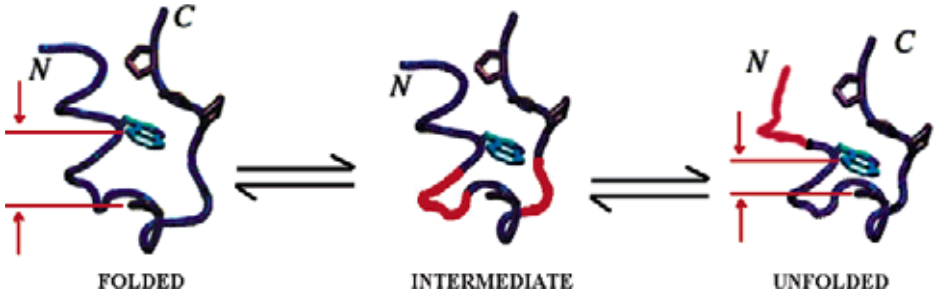

Figure 8. A schematic representation of Trp-cage's temperature dependent conformational changes.

at ~20 °C, which signals a minimum water exposure at this temperature. Thus, there is a unique structure at ~20 °C which appears to melt at higher and lower temperatures. According to the 229 nm Raman spectra the Trp (indole's N−H group) does not hydrogen bond at any temperature. Furthermore, the $C_2-C_3-C_\beta-C_\alpha$ (χ^2) dihedral angle appears constant over the 4−70 °C temperature interval. These results taken together indicate that much of the Trp-cage's native state topology survives to higher temperatures, in agreement with the conclusions of Snow et al.[43]

Our results indicate that the thermal unfolding of Trp-cage involves at least two uncoupled steps involving an intermediate state (Figure 8). The sequence of events leading to the unfolded/non-native state of Trp-cage is as follows:

(1) As the temperature is increased from 4 to 20 °C, Trp-cage adopts a compact, intermediate conformation that better shields the Trp side chain from water. The 204 nm excited C_α-H bending band does not show any significant change in intensity, indicating no change in the α-helical content. The first unfolding step may involve conformational changes around the two, glycine rich, turn/mobile regions: residues 9−10 and 15−17 (shown red in Figure 8) to form a tight core around the Trp to better shield it from the aqueous environment.

(2) As the temperature is further increased from 20 to 70 °C, the Trp intensities monotonically decrease, indicating an increased solvent exposure of the Trp ring. However, at 70 °C the Trp intensity is still 6% greater than it was at 4 °C, signifying that only a partial melting of the compact, intermediate state has occurred.

(3) The Tyr cross sections do not decrease with temperature. This suggests a decreased excitonic interaction-induced hypochromic shift, which suggests movement of Tyr away from the proline(s).

(4) During the same temperature interval the 204 nm excited AmII′ band undergoes a slow, monotonic decrease in intensity indicating a gradual increase in the Trp-proline excitonic interactions.

(5) During this temperature increase from ~20−70 °C, the $C_\alpha-H$ bending band intensity increases indicating a loss of helicity with increasing temperature.

Thus, our results in the 30−70 °C temperature interval indicate a more global conformational change which partially melts the α-helix, while the proline imide bond(s) of polyproline and/or the 3_{10} helix either align and/or brought closer to the Trp. The Tyr side chains appear to move away from the proline. The partial melting of the α-helix may allow the proline-Trp complex to open more easily to the solvent.

It should be noted that at higher temperatures, Neidigh et al.[33] noted increasingly negative chemical shift deviations for the δ3 proton of Pro_{12} and α3 of Gly_{11}. This result was rationalized by arguing that the residual high-temperature hydrophobic cluster between Trp_6 and Pro_{12} placed these two protons further into the shielding region than their location in the native state.[33] This indicates that the Gly_{11}-Pro_{12}-Trp_6 distances decrease with increasing temperature. The conclusion drawn from the NMR study agrees with our UV Raman study.

The UVRR data indicate that temperature dependence of the Trp-cage conformation involves a continuous conformational evolution with only partial helix melting at temperatures even as high as 70 °C. A straightforward interpretation of these data is that Trp-cage melts from a 20 °C maximally compact state to molten globulelike states at both higher and lower temperatures. Thus, we invoke cold denaturation of a maximally compact 20 °C state.[87,88] These changes apparently derive from changes in the protein−water interactions.[80,89]

Qiu et al.'s kinetic results found single-exponential decay in the 4−70 °C temperature range suggesting that Trp-cage behaves as a two-state folder.[35] However, this miniprotein does not show a clear two-state behavior in our steady-state studies. Rather it shows a continuous distribution of steady-state spectral parameters. Only the α-helix melting curve even hints of a cooperative transition. Possibly the previous kinetic results monitor only a small region of the Trp-cage which locally appears two-state. This would then argue for spatially decoupled folding even for this small peptide.

Acknowledgment. The authors would like to thank Dr. Ivat Bahar, Dr. John Vires, Prof. A. E. Roitberg, and Prof. S. J. Hagen for helpful discussions and NIH Grant 8 RO1 EB002053021 for financial support.

JA050664E

(87) Andersen, N. H.; Cort, J. R.; Liu, Z.; Sjoberg, S. J.; Tong, H. *J. Am. Chem. Soc.* **1996**, *118*, 42, 10309−10310.
(88) Privalov, P. L.; Griko, Y. V.; Venyaminov, S. Y.; Kutyshenko, V. P. *J. Mol. Biol.* **1986**, *190*, 487−498.
(89) Urry, D. W. *J. Phys. Chem. B* **1997**, *101*, 51, 11007−11028.